JOURNAL OF MATERIALS SCIENCE 12 (1977) 215–218

The indentation of hard metals: the role of residual stresses

C. J. STUDMAN*, J. E. FIELD
Physics and Chemistry of Solids, Cavendish Laboratory, Madingley Road, Cambridge, UK

Experimental evidence to support Johnson's [6] analysis of the residual surface stress distribution produced in a flat surface by a spherical indenter is presented. The theory suggests that high residual stresses develop just outside the contact area as a result of the superposition of elastic unloading stresses onto the stresses at maximum load when the specimen has deformed plastically. The experiments involved the use of a semi-brittle steel, sufficiently hardened so that, while tensile stresses in the surface produced cracks, the substrate deformed plastically under the triaxial stress system beneath the indenter. Radial cracks produced by the indenter frequently extended after load removal, implying the presence of the high tensile circumferential residual stresses predicted by the theory. This work and recent studies of indentation loading of glasses show that there are important situations where residual stresses can contribute to their failure and wear.

1. Introduction

Over the past few years there has been considerable interest in the behaviour of, and stress distributions in, non-conforming surfaces under dynamic loading. The subject has many important applications, particularly with regard to bearing failures caused by contact fatigue [1, 2], and the failure of steel rails and gear teeth [3]. A simplified situation, the repeated indentation of a flat test surface by a hard sphere, can frequently give a reasonable indication of the behaviour of materials in more complex geometries. In this, as in other cases, a number of mechanisms have been suggested to explain the eventual failure of the surface [3, 5]. Johnson [6] attempted to show how tensile residual surface stresses can arise outside the area of contact, by considering the stresses produced by unloading a specimen whose substrate has deformed plastically during loading. His analysis implied that high tensile residual stresses could be produced by a single quasistatic indentation. This paper offers experimental evidence that this is so. A semi-brittle water-quenched carbon steel, which failed by brittle fracture under uniaxial tension but which deformed plastically under suitable triaxial loading, was used to reveal tensile surface stresses.

2. Theory

2.1. Surface stresses during loading

The perfect elastic problem of a sphere indenting a flat surface was solved by Hertz [7]. The solutions for the radial and the circumferential stresses outside the circle of contact are

$$\sigma_r = -\sigma_\theta = \frac{(1-2\nu)P}{2}\frac{a^2}{r^2} \quad (r>a) \qquad (1)$$

where P is the mean contact pressure, and r is the distance from the axis of the indenter. The radius of the circle of contact, a is given by

$$a^3 = \tfrac{3}{4}FR\left\{\frac{1-\nu^2}{E}+\frac{1-\nu'^2}{E'}\right\} \qquad (2)$$

where ν, ν' and E, E' are the Poisson's ratio and Young's modulus of the specimen and indenter respectively, R is the relative radius of curvature of the two surfaces, and F is the applied load. Thus σ_r is a maximum and tensile at $r=a$,

*Present address: Agricultural Engineering Department, Massey University, New Zealand.

causing the well-known cone crack in glass [8, 9].

In contrast, when there is significant plastic flow, the surface stresses are not known and empirical methods must be used to obtain values. By considering plastic strain rates for loads, F, much in excess of the load for first plastic flow, F^*, Johnson [6] found that just outside the contact area, σ_θ was at the yield point Y, while σ_r was nearly zero. Further away from the contact area σ_r initially became more compressive, while σ_θ decreased.

It is clear that at both low and high applied loads the maximum tensile surface stresses occur at $r = a$. In the intermediate range σ_r and σ_θ at this radius may be plotted schematically as in Fig. 1. Initially the surface stresses deviate only very slightly from the elastic analysis [10, 11] and therefore σ_r continue to rise with applied load.

The maximum value of σ_r is at point A, while σ_θ does not become of similar magnitude until point B is reached.

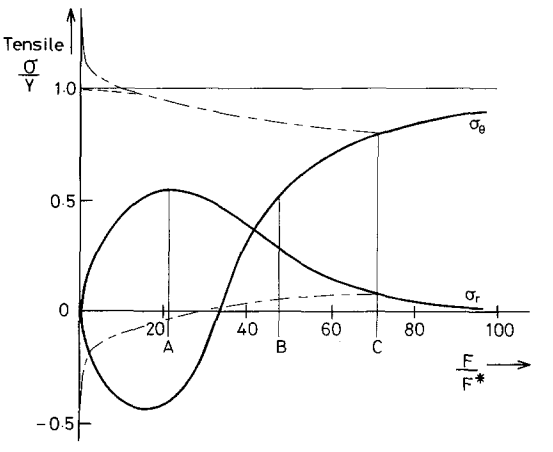

Figure 1 Hypothetical plot of surface radial stress, σ_r, and circumferential stress, σ_θ, at $r = a$. A and B indicate loads where σ_r and σ_θ respectively become sufficiently high to cause cracking. Full lines denote loading curves, while chained lines represent unloading from an arbitrary point C for fully elastic behaviour. Dashed line indicates curve for non-elastic behaviour.

2.2. Surface stresses during unloading

Johnson [6] suggested that the residual stresses after unloading can be obtained by subtracting the elastic stress system arising from the applied pressure, from the stresses calculated at maximum load. Thus on unloading, the stresses at $r = a$ are, from Equation 1

$$\sigma_r = \sigma_{rm} - \tfrac{1}{2}(1-2\nu)(P_m - P) \quad (3)$$

$$\sigma_\theta = \sigma_{\theta m} + \tfrac{1}{2}(1-2\nu)(P_m - P) \quad (4)$$

where σ_{rm} and $\sigma_{\theta m}$ are the radial and circumferential surface stresses respectively and P_m is the average pressure over the area of contact, all at maximum load. These curves are also plotted in Fig. 1, for an arbitrary value of P_m (corresponding to point C on Fig. 1). For large values of F/F^*, the values of σ_r and σ_θ after complete unloading may be obtained from Equations 3 and 4 by inserting Johnson's values of $\sigma_{rm} = 0$, $\sigma_{\theta m} = Y$ and using $P_m = 2.5Y$ and $\nu = 0.3$. This gives

$$\sigma_r = -0.5Y \quad (5)$$

$$\sigma_\theta = 1.5Y. \quad (6)$$

It is clearly not possible in practice for σ_θ to exceed Y, and thus some non-elastic behaviour must occur during unloading as Johnson pointed out [6, 12]. This effect is included in Fig. 1. However, the analysis clearly suggests that high tensile circumferential stresses are produced during unloading at $r = a$.

3. Experimental

10 mm thick specimens of an EN44 B carbon steel were heat-treated and stress relieved to produce a hardness of about 800 DPN. They were then carefully polished to produce a highly reflective surface. Full details of the process are given by Studman [13]. The indenters were tungsten carbide spheres and loads were applied at constant stress rate, usually 250 N sec^{-1}, using a hydraulic testing machine. The maximum load was held constant for 20 sec, and then the applied load was reduced at approximately half the loading rate. The specimen was removed, examined for damage, and photographed. The specimens were re-examined a few minutes later and rephotographed.

4. Results

Radial and circumferential cracks were produced by the indenter at sufficiently high loads (Fig. 2a). More radial cracks were found for higher values of F/F^* (Fig. 2b). It was found that radial cracks often continued to extend after load removal, for example, a significant part of the radial crack growth of Fig. 2a occurred after load removal. Fig. 3 shows an indentation at times of 2 and 8 min after load removal. In this time interval crack

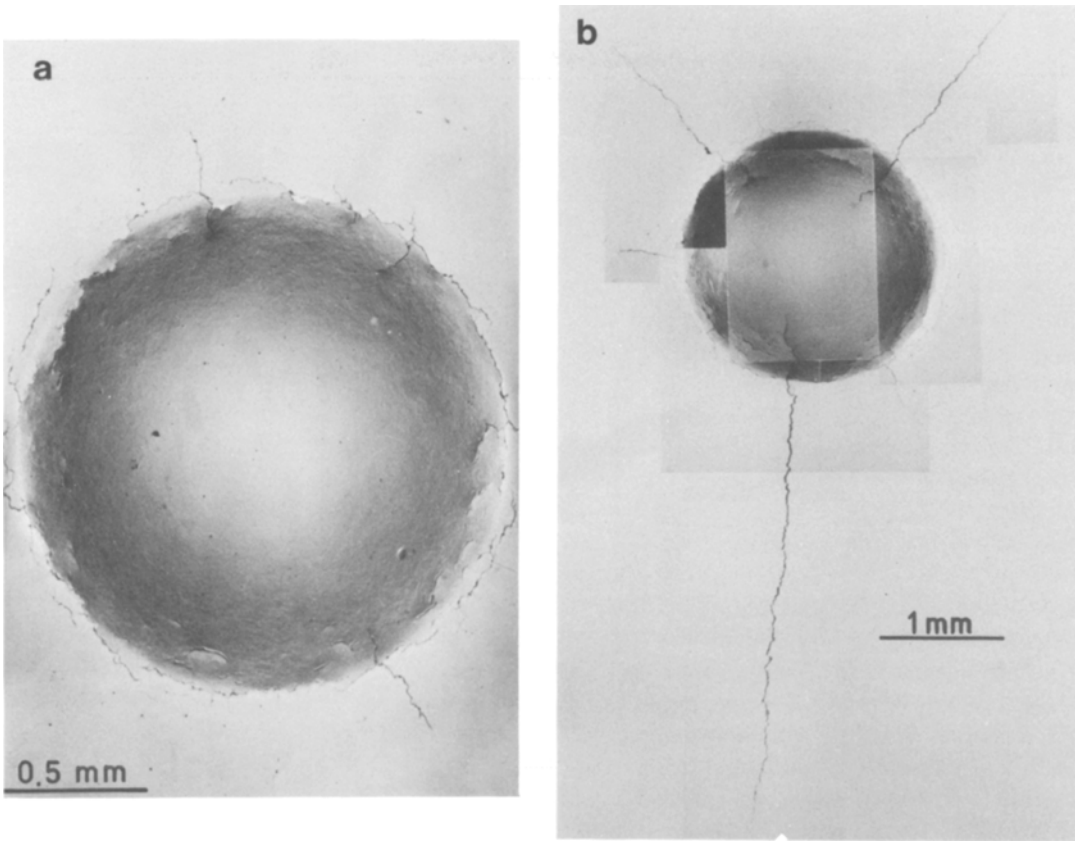

Figure 2 Examples of radial and circumferential cracking caused by a 10 mm diameter tungsten carbide indenter. Both photographs were taken some time after the experiment. (a) Maximum load 15 kN, $F/F^* = 30$, $a_m = 0.84$ mm. (b) Maximum load 25 kN, $F/F^* = 50$, $a_m = 1.02$ mm. Note increase in radial cracking.

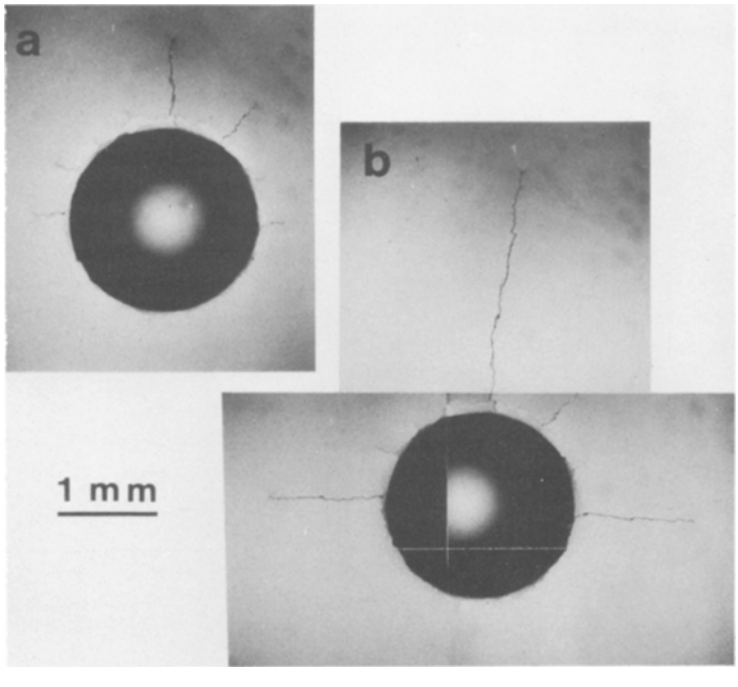

Figure 3 Indentation with 10 mm diameter sphere showing extension of radial cracks after load removal. Maximum applied load was 25 kN: (a) within 2 min of end of loading; (b) 8 min later.

extensions of up to 2 mm have taken place. In some cases radial cracks continued to extend over a period of a few days. No evidence was found of the extension of circumferential cracks following load removal.

5. Discussion

Circumferential or radial cracking is likely when σ_r or σ_θ respectively are highly tensile. During loading the former can occur near point A of Fig. 1, while radial cracking may occur only at loads near or beyond B. Circumferential cracking would therefore be expected at low loads, changing to predominantly radial cracking at high loads, as found in the experiments. If the specimen is unloaded from point C of Fig. 1, the unloading curves are followed, and further radial cracking can occur. No direct observations of crack growth during unloading were possible: efforts to monitor stress wave emission from the specimens, as reported by Wilshaw and Swindlehurst [14] for glass, proved unsuccessful because of the difficulty of distinguishing between emissions due to cracking and plastic deformation. However, on completion of unloading, the theory predicts that σ_θ reaches a maximum, and the radial cracks will thus be in a highly unstable state. In the first few minutes after unloading crack extensions of a few millimeters were common. However, crack growth could also continue over a period of days, and this is probably a combination of the residual stresses and atmospheric effects; Uhlig [15], for example, has shown the importance of atmospheric water vapour on crack growth in steels.

Recent research on the indentation loading of glasses has also shown that there are situations where residual stresses contribute to the failure. For example, Studman [13] using spherical tungsten carbide indenters (diameter ~ 0.4 mm) and Lawn and co-workers [16, 17] using pointed diamond indenters have shown that localized inelastic deformation can occur beneath the indenter. On unloading, residual stresses associated with this deformation, produced lateral vent cracking.

The results of the present paper, and those on glass failure, have practical importance in understanding the deformation and wear of materials which, although basically brittle, exhibit plastic or some other form of inelastic deformation, when indented.

Acknowledgements

This work was completed partly at the Cavendish Laboratory, Cambridge, and partly at the National Institute of Agricultural Engineering, Silsoe, Bedfordshire. We thank the S.R.C. for a grant to the Laboratory. C.J.S. thanks the A.R.C. for support during the period of research, and the director of the N.I.A.E. for permission to publish these results.

References

1. D. SCOTT, *Wear* **25** (1973) 199.
2. N. TSUSHIMA, H. MURO and K. NUNOME, *ibid* **25** (1973) 345.
3. E. GERVAIS and H. J. McQUEEN, *J.I.S.I.* **210** (1972) 189.
4. J. C. TYLER, R. A. BURTON and P. M. KU, *Trans. ASLE* **6** (1963) 255.
5. S. W. PINEGIN, A. W. ORLOV and V. M. GOODCHENKO, Proceedings of the 2nd Conference on dimensioning and strength calculation, Budapest (Hungarian Academy of Sciences, 1965) p. 411.
6. K. L. JOHNSON, in "Engineering Plasticity" (Cambridge University Press, 1968) p. 341.
7. H. HERTZ, *J. Reine Angew Math.* **92** (1881) 156.
8. F. C. FRANK and B. R. LAWN, *Proc. Roy. Soc. A* **299** (1967) 291.
9. T. R. WILSHAW, *J. Phys. D: Appl. Phys.* **4** (1971) 1567.
10. C. HARDY, C. N. BARONET and G. V. TORDION, *Int. J. Numerical Methods in Engng.* **3** (1971) 451.
11. D. TABOR, *Proc. Roy. Soc. A* **192** (1948) 247.
12. K. L. JOHNSON, *Nature* **199** (1963) 1282.
13. C. J. STUDMAN, PhD Thesis, University of Cambridge (1974).
14. T. R. WILSHAW and W. E. SWINDLEHURST, Acoustic emission conference (Institute of Physics, London 1972).
15. H. H. UHLIG, "Fracture – an Advanced Treatise", Vol. 3, edited by H. Liebowitz, Academic Press, New York, 1971) p. 646.
16. B. R. LAWN and M. V. SWAIN, *J. Mater. Sci.* **10** (1975) 113.
17. B. R. LAWN and E. G. FULLER, *ibid*, **10** (1975) 2016.

Received 3 June and accepted 7 July 1976.